Journal of Nanobiotechnology

RESEARCH

Open Access

IL-7 promotes mRNA vaccine-induced long-term immunity

Lingli Wang[1,2,3,4†], Jiawu Wan[1,2,3,4†], Wenna He[1,2,3,4], Zongmei Wang[1,2,3,4], Qiong Wu[1,2,3,4], Ming Zhou[1,2,3,4], Zhen F. Fu[1,2,3,4] and Ling Zhao[1,2,3,4*]

Abstract

Messenger RNA (mRNA) vaccines are a key technology in combating existing and emerging infectious diseases. However, improving the immunogenicity and durability of mRNA vaccines remains a challenge. To elicit optimal immune responses, integrating antigen-encoded mRNA and immunostimulatory adjuvants into a single formulation is a promising approach to enhancing the efficacy of mRNA vaccines. Here, we report an adjuvant strategy to enhance the efficacy of mRNA vaccines by co-loading mRNA encoding the antigen (rabies virus glycoprotein, RABV-G) and mRNA encoding IL-7 into lipid nanoparticles, achieving co-delivery to the same antigen-presenting cells. A single immunization with G&IL-7 mRNA vaccine elicited robust humoral immune responses in mice and conferred complete protection against RABV challenge. Notably, the high levels of neutralizing antibody induced by the G&IL-7 mRNA vaccine were maintained for at least 6 months, providing mice with long-term significant and complete protection against RABV. Additionally, IL-7 also enhanced antibody responses against the SARS-CoV-2. These data demonstrate that IL-7 is a potent mRNA vaccine adjuvant that can provide the required immune stimulation in various mRNA vaccine formulations.

Keywords IL-7, mRNA vaccine, Adjuvant, Lipid nanoparticles, Long-term protection

†Lingli Wang and Jiawu Wan contributed equally to this work.

*Correspondence:
Ling Zhao
zling604@outlook.com; lingzhao@mail.hzau.edu.cn
Full list of author information is available at the end of the article

Graphical Abstract

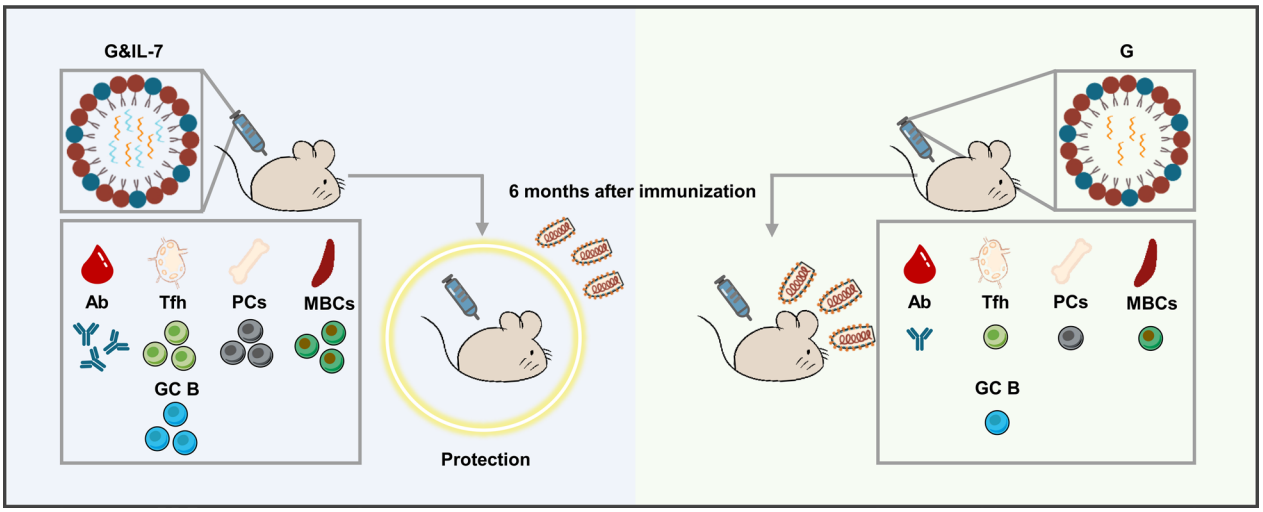

Introduction

Rabies is a fatal zoonotic disease with a mortality rate close to 100%, caused by the neurotropic rabies virus (RABV) [1, 2]. Prevention of RABV following virus exposure relies on rapid antibody-mediated neutralization of RABV before it enters the central nervous system [3]. This includes the use of RABV immune globulin purified from vaccinated horses or human donors, as well as up to five doses of RABV vaccine [4]. Approximately 17 million people are vaccinated and treated after exposure to RABV each year [4]. While many vaccines have proven highly successful in preventing RABV, the demand for multiple doses and high costs have led to incomplete protection in endemic areas, resulting in around 60,000 deaths worldwide annually [2, 5–7]. For many significant human pathogens, including severe acute respiratory syndrome coronavirus 2 (SARS-CoV-2) and human immunodeficiency virus 1 (HIV-1), vaccine-induced protective antibody responses have been proven challenging [8–10]. One of the current focuses of RABV vaccine research has shifted from inducing effective immunity to reducing costs while maintaining sufficient immunogenicity and streamlining vaccination procedures [11]. Although multi-dose regimens can enhance immune responses and duration, they also increase the complexity and cost of vaccination programs, as well as the likelihood of adverse reactions, making them suboptimal strategies. Therefore, the development of single-dose, highly immunogenic RABV vaccines is crucial, particularly for developing countries, as it would help alleviate the financial burden on local governments for rabies prevention.

Messenger RNA (mRNA) vaccines have achieved tremendous success in the pandemic of SARS-CoV-2 [12, 13]. Delivery of RABV-G mRNA vaccine via lipid nanoparticles (LNPs) has improved its immunogenicity in rodents and non-human primates (NHPs) [14]. The first clinical trial of this formulation tested safety and serum conversion following administration of one or two low doses (1, 2, and 5 μg), revealing that 100% of participants induced neutralizing titers above the World Health Organization (WHO) threshold in the two-dose groups [15, 16]. However, compared to the three-dose Rabipur vaccine (a rabies inactivated vaccine), the levels were lower and kinetics delayed, indicating the need for improving mRNA vaccine dosing strategies to surpass Rabipur [17]. Various measures have been adopted to enhance the immunogenicity of mRNA vaccines, including improving delivery systems, targeted delivery, using circular RNA vaccines, and employing adjuvants. Our previous work has demonstrated that using lipopolyplex nanoparticles delivery systems and employing circular RNA vaccines with higher stability can effectively enhance the immunogenicity of mRNA vaccines [11, 18]. The team led by Satoshi Uchida effectively enhanced the efficacy of mRNA vaccines by integrating immunostimulatory adjuvants into the mRNA chain through RNA engineering [19]. Additionally, researchers have induced robust immune responses against variants of the novel coronavirus by using manganese-adjuvanted mRNA

vaccines [20]. These studies collectively demonstrate the tremendous potential for enhancing mRNA vaccines.

As a cytokine, interleukin-7 (IL-7) plays a crucial role in the proliferation and differentiation of lymphocyte subsets, particularly T cells and B cells [21]. Specifically, exogenous IL-7 has been found to enhance humoral immunity by promoting the development of T follicular helper (Tfh) cells [21]. Tfh cells provide help to B cells, inducing the generation of high-affinity antibodies in germinal centers (GCs) [22]. Therefore, IL-7 is considered a key cytokine for inducing Tfh cell production and enhancing antibody responses. Particularly, a recent study discovered that IL-7 pretreatment significantly enhances the protein expression capacity of mRNA in T cells, which plays a critical role in enhancing mRNA immunogenicity [23]. These findings underscore the potential of IL-7 as a novel adjuvant in enhancing the immunogenicity of mRNA vaccines.

In this study, we employed IL-7 as a stimulatory adjuvant to enhance the immune response, co-delivering IL-7 mRNA and RABV G mRNA in LNPs for synergistic immunization. Following a single-dose vaccination of this vaccine in mice, compared to vaccines without IL-7, it exhibited the ability to stimulate higher levels of RABV virus-neutralizing antibody by promoting germinal center reactions. It also provided protection against RABV challenge in mice for up to 6 months. Meanwhile, when using the SARS-CoV-2 as a model, IL-7 effectively enhanced the antibody response induced by S mRNA encoding the spike (S) protein of the SARS-CoV-2. These findings suggest that IL-7 encoded by mRNA is a promising candidate adjuvant for mRNA vaccines against emerging and re-emerging infectious pathogens.

Results

The design and characterization of an mRNA vaccine expressing both RABV-G and IL-7

Having previously demonstrated the feasibility of utilizing the glycoprotein derived from the RABV as an antigen for mRNA-based vaccines in human subjects [17], we have developed an mRNA vaccine encoding the glycoprotein (G) of the RABV. Additionally, IL-7 mRNA as an adjuvant has been introduced, accompanied by the utilization of the modified nucleoside N^1-methylpseudopyrimidine (Fig. 1A). Capillary electrophoresis and agarose gel electrophoresis analysis confirmed that the in vitro-transcribed mRNA exhibited high purity and integrity (Fig. S1A and B). To extend and facilitate efficient antigen expression [24], G mRNA and IL-7 mRNA were furthermore co-encapsulated in LNPs for vaccination, termed as G&IL-7 mRNA (Fig. 1B). The encapsulation efficiency of the LNPs was determined, and the analysis revealed that the LNP formulation achieved an encapsulation efficiency of 86.1%. Transmission electron microscopy (TEM) analysis revealed the presence of an electron-dense core in LNPs encapsulating mRNA (Fig. 1C), while dynamic light scattering analysis in PBS characterized the particle size of the LNPs (Fig. 1D). Subsequently, following the transfection of HEK-293T cells with LNP-encapsulated G mRNA, IL-7 mRNA or G&IL-7 mRNA, the expression of G and IL-7 were confirmed (Fig. 1E and Fig. S1C).

IL-7 enhances the RABV mRNA vaccine-induced antibody titers

The dose of G mRNA used in this study was selected based on previously experiments conducted in our laboratory, as well as data from published research on RABV mRNA vaccines [18, 25]. To determine the adjuvant effect of IL-7 mRNA on the immunogenicity of the RABV mRNA vaccine, we first conducted an experiment comparing the efficacy of co-encapsulating G and IL-7 mRNA in a single LNP versus separately encapsulating them in different LNPs followed by co-injection. The results showed no significant difference in the levels of RABV virus-neutralizing antibody (VNA) titer induced by the two strategies (Fig. S2). Given the similar immune response results, the co-encapsulation strategy was chosen, as it simplifies the vaccine production process and reduces costs. IL-7 mRNA was screened at doses of 0.5 μg, 2.5 μg, and 5 μg, each co-encapsulated with G mRNA at a fixed dose of 2.5 μg in LNPs (Fig. 2A). These LNP-encapsulated RABV mRNA vaccines were administered to mice, and blood samples were collected weekly for 6 weeks to measure VNA titers. The results showed that, compared to the control group receiving only G mRNA, the RABV mRNA vaccine containing 2.5 μg and 5 μg of IL-7 mRNA produced higher levels of VNA titers. However, there was no significant difference in VNA titers levels between the two doses of IL-7 mRNA (Fig. 2B). Therefore, 2.5 μg of IL-7 mRNA was chosen as the adjuvant dose for subsequent experiments. Using G mRNA, G&IL-7 mRNA or inactivated rabies vaccine (ITV) for immunization of mice, serum samples were collected and VNA titers levels were monitored for up to 6 months (Fig. 2C). The results showed that IL-7 mRNA as an adjuvant enhanced the immunogenicity of the RABV mRNA vaccine throughout the 6-month period. Moreover, IL-7 mRNA prolonged the peak of VNA titers from the fourth week to the fifth week, sustaining it at a higher level than the peak observed in the G mRNA and ITV vaccine group during the fourth week for a duration of seventh week (Fig. 2D).

To further evaluate the quality of antibody responses, we performed enzyme-linked immunosorbent assay (ELISA) to measure IgG, IgG1, IgG2a, and IgG2b

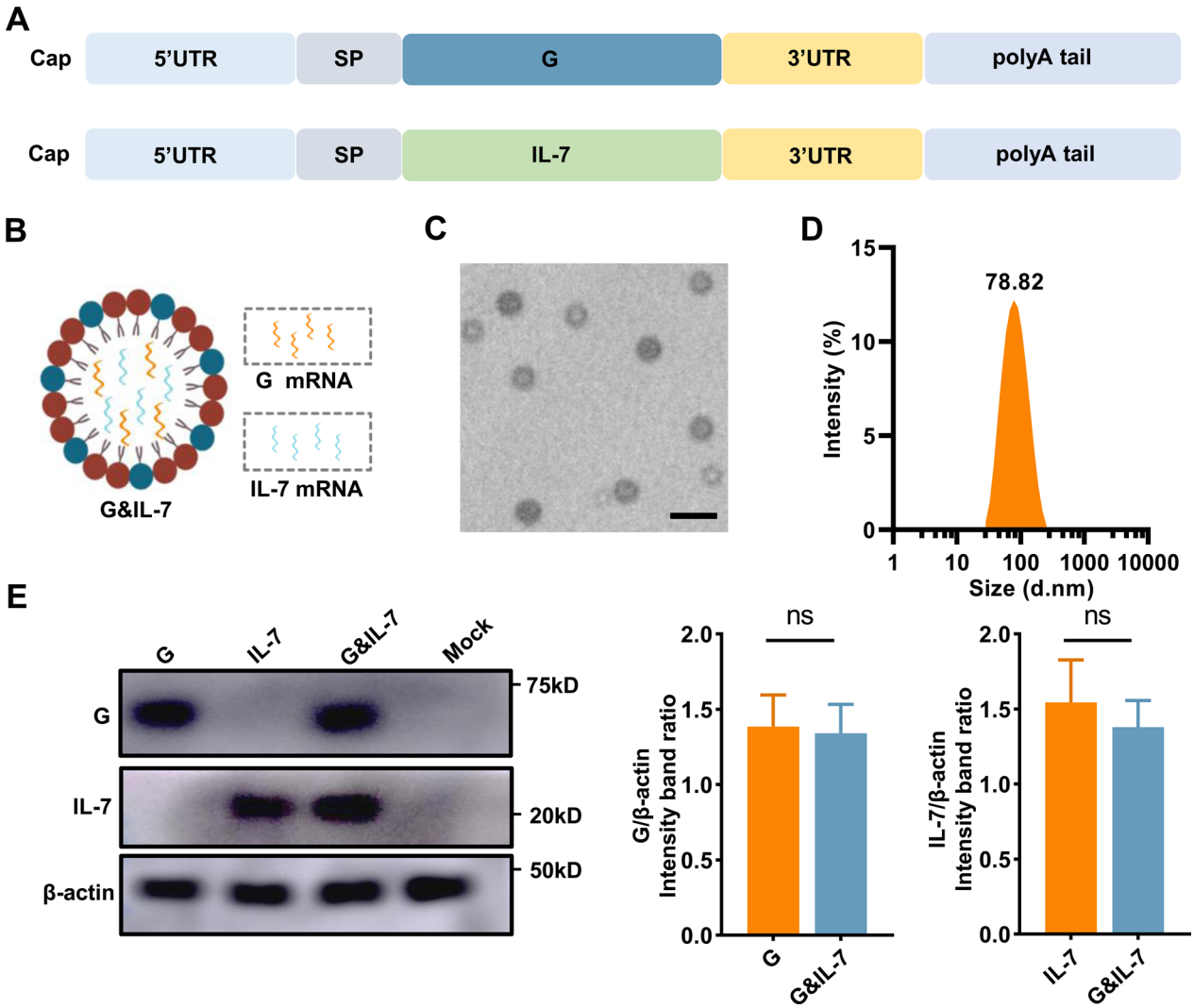

Fig. 1 The design and characterization of a RABV mRNA vaccine expressing IL-7. **A** A schematic diagram of nucleoside-modified mRNA encoding G and IL-7. SP: signal peptide. **B** A schematic diagram illustrating the co-encapsulation of IL-7 mRNA as an adjuvant with G mRNA in LNPs for vaccination. **C** A representative transmission electron microscopy (TEM) image of LNPs in solution after mRNA encapsulation. Scale bar, 100 nm. **D** Particle size of LNPs measured using dynamic light scattering (DLS). **E** HEK-293T cells were transfected with LNP-encapsulated G mRNA (1 μg), IL-7 mRNA (1 μg) or G&IL-7 mRNA (1 μg G mRNA + 1 μg IL-7 mRNA). After 24 h, Western blotting was performed to measure the expression levels of G and IL-7 in the cell lysates (n = 3)

levels in the serum (Fig. 2E–H). Consistent trends were observed across IgG and other antibody isotypes, indicating that the addition of IL-7 mRNA as an adjuvant led to increased levels of IgG and other antibody isotypes induced by the G mRNA.

IL-7 induces the reprogramming of transcriptome in inguinal lymph nodes

Inguinal lymph nodes are the primary sites where adaptive immune responses are generated. When exposed to foreign pathogens or antigens, immune cells gather in the inguinal lymph nodes, interact with antigens, and proliferate to generate immune responses [22, 26]. To investigate whether the expression of IL-7 affects the microenvironment of inguinal lymph nodes, we studied the transcriptomic changes in inguinal lymph nodes of mice vaccinated with G&IL-7 mRNA vaccine. The principal component analysis (PCA) plot demonstrated significant differences between the IL-7 mRNA vaccination group and the control group (Fig. 3A), with 103 genes upregulated and 229 genes downregulated (Fig. 3B), indicating substantial transcriptional changes in mouse inguinal lymph nodes following IL-7 mRNA vaccination.

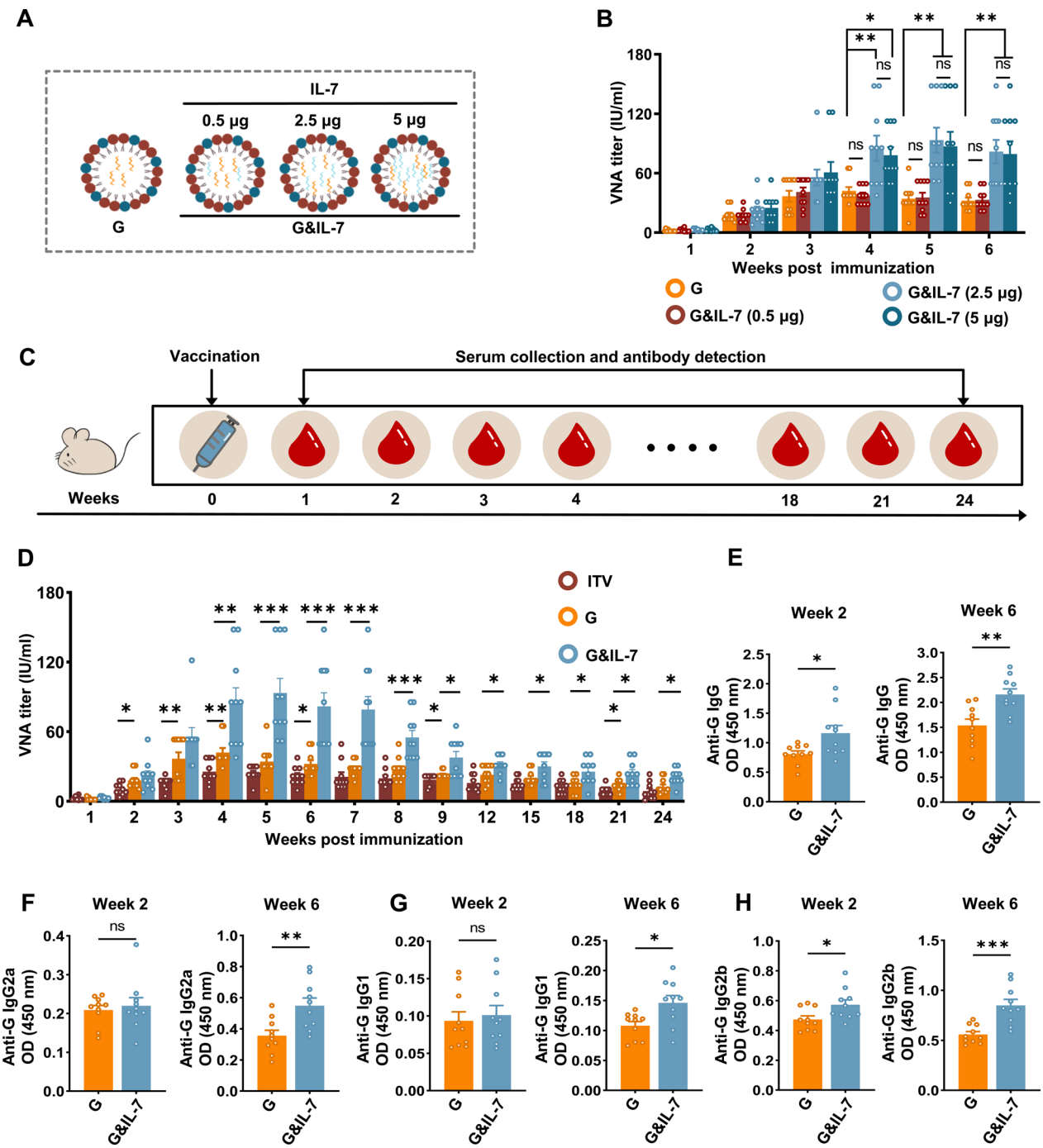

Fig. 2 IL-7 enhances mRNA vaccine-induced antibody production in mice. **A** Schematic diagram of IL-7 mRNA (0.5 μg, 2.5 μg, and 5 μg) as an adjuvant co-encapsulated with 2.5 μg of G mRNA in LNPs. **B** Mice were administered G mRNA encapsulated with varying concentrations of IL-7 mRNA. RABV virus-neutralizing antibody (VNA) titers were assessed using fluorescent antibody virus neutralization assays (n = 10). **C** Mice were immunized via intramuscular injection with G mRNA, G&IL-7 mRNA, or the ITV vaccine. Serum samples were collected starting from week 1 post immunization and continued until week 24. **D**–**H** VNA titers were assessed via FAVN assays. IgG, IgG1, IgG2a, and IgG2b levels in the serum were measured by ELISA (n = 10)

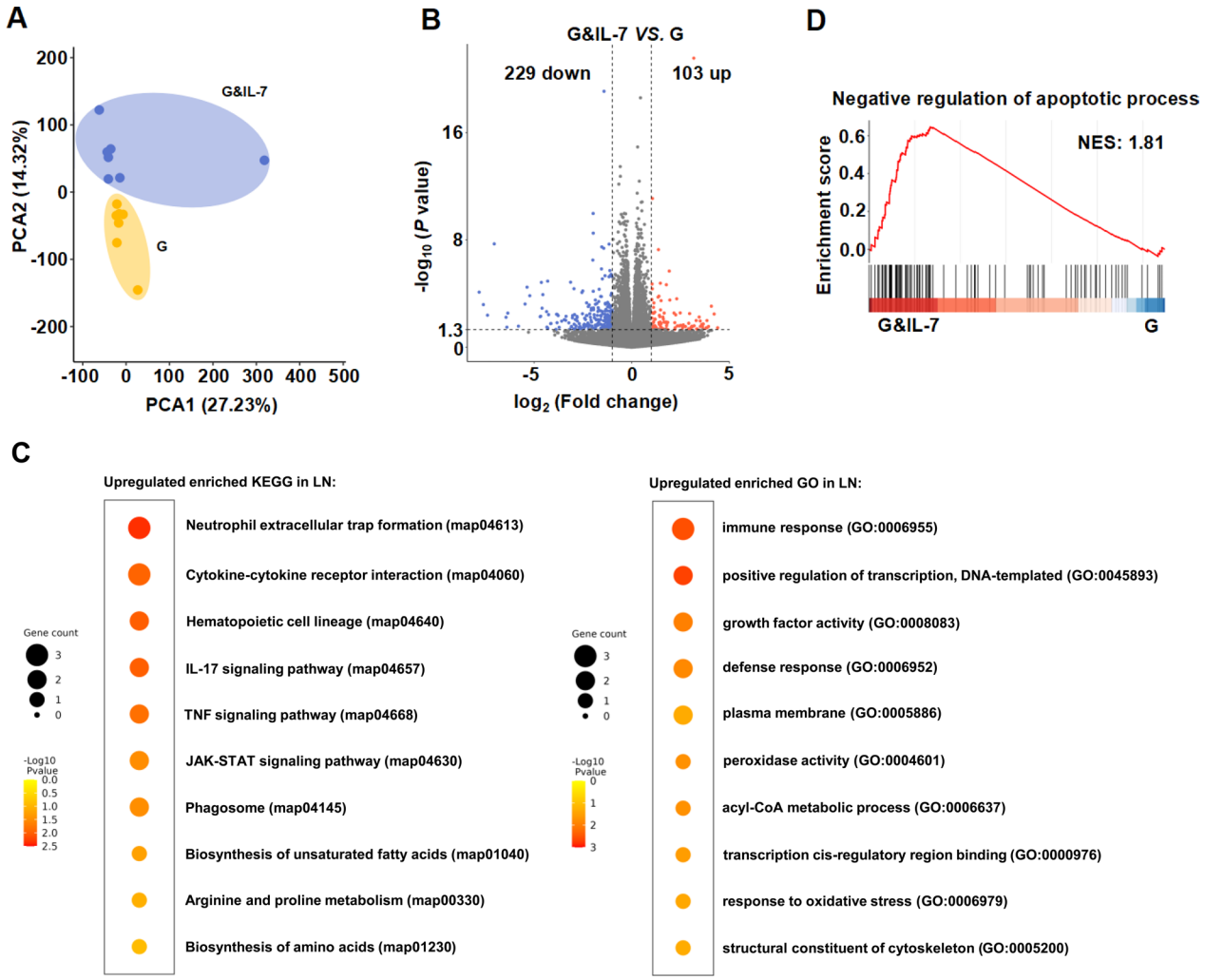

Fig. 3 Transcriptome analysis of LNs reveals distinct immune responses between IL-7 expression and control mice. **A** The PCA model plot of transcriptomic profiles from the inguinal lymph nodes (LNs) of mice (n = 7) inoculated with G&IL-7 mRNA and G mRNA. PCA Plot showing the global differences between IL-7 expression and control groups. **B** Volcano plots of differentially expressed genes between different groups. The red dots represent genes that are upregulated, the blue dots represent genes that are downregulated, and the gray dots represent genes that are not different. FDR < 0.01, | log2 (fold change) | > 1. **C** KEGG and GO enrichment analysis of differentially expressed genes. The data are represented as circles, where the size indicates the gene count for that particular process, and the color represents the −Log10 p-value calculated with one-sided Fisher's Exact test with Benjamini–Hochberg correction. **D** GSEA pathway enrichment analysis of the identified differentially expressed genes present in the genome G&IL-7 vs G with negative regulation of apoptotic process path. *PCA* principal component analysis, *KEGG* Kyoto Encyclopedia of Genes and Genomes, *GO* Gene Ontology, *FDR* False Discovery Rate

After IL-7 mRNA vaccination, pathways related to adaptive immunity, oxidative stress, amino acid synthesis, fatty acid metabolism, neutrophil extracellular trap formation, and inflammatory responses (including TNF signaling pathway, IL-17 signaling pathway, JAK-STAT signaling pathway) were significantly enriched (Fig. 3C). IL-7 primarily regulates the development of B cells, T cells, and dendritic cells through pathways such as JAK-STAT and PI3K-Akt [27–29]. However, although PI3K-Akt appeared to be enriched here, it was not significant. To investigate the potential involvement of the JAK-STAT pathway in response to IL-7 stimulation, we performed quantitative RT-PCR to assess the expression of key genes in this signaling pathway. The results showed a significant upregulation of JAK1, STAT5A, STAT5B, SOCS1, and SOCS2, suggesting the involvement of the JAK-STAT pathway (Fig. S3A). To further verify JAK-STAT pathway activation, Western Blot (WB) analysis was employed to confirm the phosphorylation of JAK1 and STAT5, which are commonly regarded as markers indicative of this pathway's activation [30–32]. Experimental results indicated

that phosphorylation levels of JAK1 and STAT5 in the G&IL-7 group were significantly upregulated compared to the G group, thus confirming the activation of the JAK-STAT pathway at the protein level (Fig. S3B). Additionally, pathways including transcription, anti-apoptosis, cellular cytoskeleton components, cellular membrane, and phagosome also showed significant enrichment (Fig. 3C, D). Overall, these results indicate that IL-7 vaccination alters the overall transcriptional profile of mouse inguinal lymph nodes.

IL-7 promotes the proliferation of Tfh cells, GC B cells and PCs in mice

T follicular helper (Tfh) cells have the specialized ability to migrate towards Germinal Centers (GCs), which are structures densely populated by highly proliferative Germinal Center B (GC B) Cells [33]. They play a critical role in producing enduring and high-affinity B cell responses [34]. Hence, further investigation was conducted to explore the function of IL-7 mRNA in the formation of Tfh cells and GC B cells. Three groups of C57BL/6 mice received immunization with G mRNA, G&IL-7 mRNA, or PBS, and the frequencies of Tfh cells (Fig. 4A and Fig. S4A) and GC B cells (Fig. 4C and Fig. S4B) in the inguinal lymph nodes were evaluated by flow cytometry at 7 days and 14 days post-immunization (dpi). Compared to the G mRNA, G&IL-7 mRNA elicited a robust population of Tfh cells (Fig. 4B) and GC B cells (Fig. 4D) at 7 and 14 dpi.

GC B cells undergo differentiation into either memory B cells (MBCs) or plasma cells (PCs) through interactions with Tfh cells, which is a crucial step in establishing immune protection [35, 36]. To assess the impact of IL-7 mRNA on PCs formation, the proportion of PCs (Fig. 4E and Fig. S4C) was evaluated using flow cytometry following immunization mice with G mRNA, G&IL-7 mRNA, or PBS. As anticipated, mice vaccinated with G&IL-7 mRNA exhibited significantly more PCs in bone marrows compared to those vaccinated with G mRNA (Fig. 4F). These findings collectively suggest that G&IL-7 mRNA vaccine boosts the generation of Tfh cells, GC B cells and PCs in mice compared to the G mRNA.

IL-7 expressing mRNA vaccine elicits robust secondary antibody responses in mice

Memory B cells (MBCs) play a crucial role in the rapid establishment of protective immunity upon re-infection [37, 38]. To evaluate the potential of IL-7 mRNA in inducing memory immunity post-immunization, mice were immunized with G mRNA, G&IL-7 mRNA, or PBS, and flow cytometry was used to assess the ratio of MBCs (Fig. 5A and Fig. S5) at 6 weeks post immunization (wpi). A substantial increase in MBCs (Fig. 5B) was observed in mice immunized with G&IL-7 mRNA compared to those that received G mRNA. To further assess the influence of IL-7 mRNA on the secondary antibody response, mice received booster immunization using the same doses as the primary immunization at 24 wpi (Fig. 5C). Two weeks after the booster immunization, the BM cells and LNs cells were collected for the evaluation of PCs (Fig. 5D and Fig. S4C) and RABV-specific antibody-secreting cells (ASCs; Fig. 5F) using flow cytometry and ELISpot assays, respectively. G&IL-7 mRNA elicited significantly higher levels of PCs (Fig. 5E) and RABV-specific ASCs (Fig. 5G) compared to G mRNA. Similarly, G&IL-7 mRNA resulted in higher levels of IgG (Fig. 5H) and VNA titers (Fig. 5I) compared to G mRNA in mice 14 days post-receiving a booster dose.

IL-7 expressing mRNA vaccine induces durable antibody production and provides long-term protection

To further determine the long-term protective efficacy of G&IL-7 mRNA in comparison with G mRNA, mice were immunized with G mRNA, G&IL-7 mRNA, or PBS. Subsequently, the mice were challenged with a lethal dose of 50 LD_{50} of the virulent RABV strain CVS-24 at 3 weeks (Fig. 6A) or 24 weeks (Fig. 6D) post immunization were performed, respectively. No deaths were observed in mice that received G&IL-7 mRNA or G mRNA 3 weeks prior to the RABV challenge, while all mice that received the placebo succumbed to rabies within 10 days (Fig. 6C). Notably, 70% and 100% of the mice in the G mRNA and G&IL-7 mRNA groups survived RABV challenge at week

(See figure on next page.)

Fig. 4 IL-7 promotes the proliferation of Tfh cells, GC B cells and PCs in mice. C57BL/6 mice were immunized with G mRNA, G&IL-7 mRNA, or PBS, respectively. **A** Representative flow cytometric plots of Tfh cells in inguinal lymph nodes (LNs) cells. At 7 and 14 dpi, LNs cells were stained with markers specific to Tfh cells ($CD4^+CXCR5^+PD\text{-}1^+$). **B** Statistical analyses were conducted on $CD4^+CXCR5^+PD\text{-}1^+$ Tfh cell plots (n = 5). **C** Representative flow cytometric plots of GC B cells in inguinal lymph nodes cells. At 7 and 14 dpi, LNs cells were stained with markers specific to GC B cells ($B220^+GL7^+CD95^+$). **D** Statistical analyses were conducted on $B220^+GL7^+CD95^+$ GC B cell plots (n = 5). **E** Representative flow cytometric plots of PCs in bone marrow (BM) cells. At 7 and 14 dpi, BM cells were stained with markers specific to PCs ($B220^{low}CD138^+$). **F** Statistical analyses were conducted on $B220^{low}CD138^+$ PCs plots (n = 5)

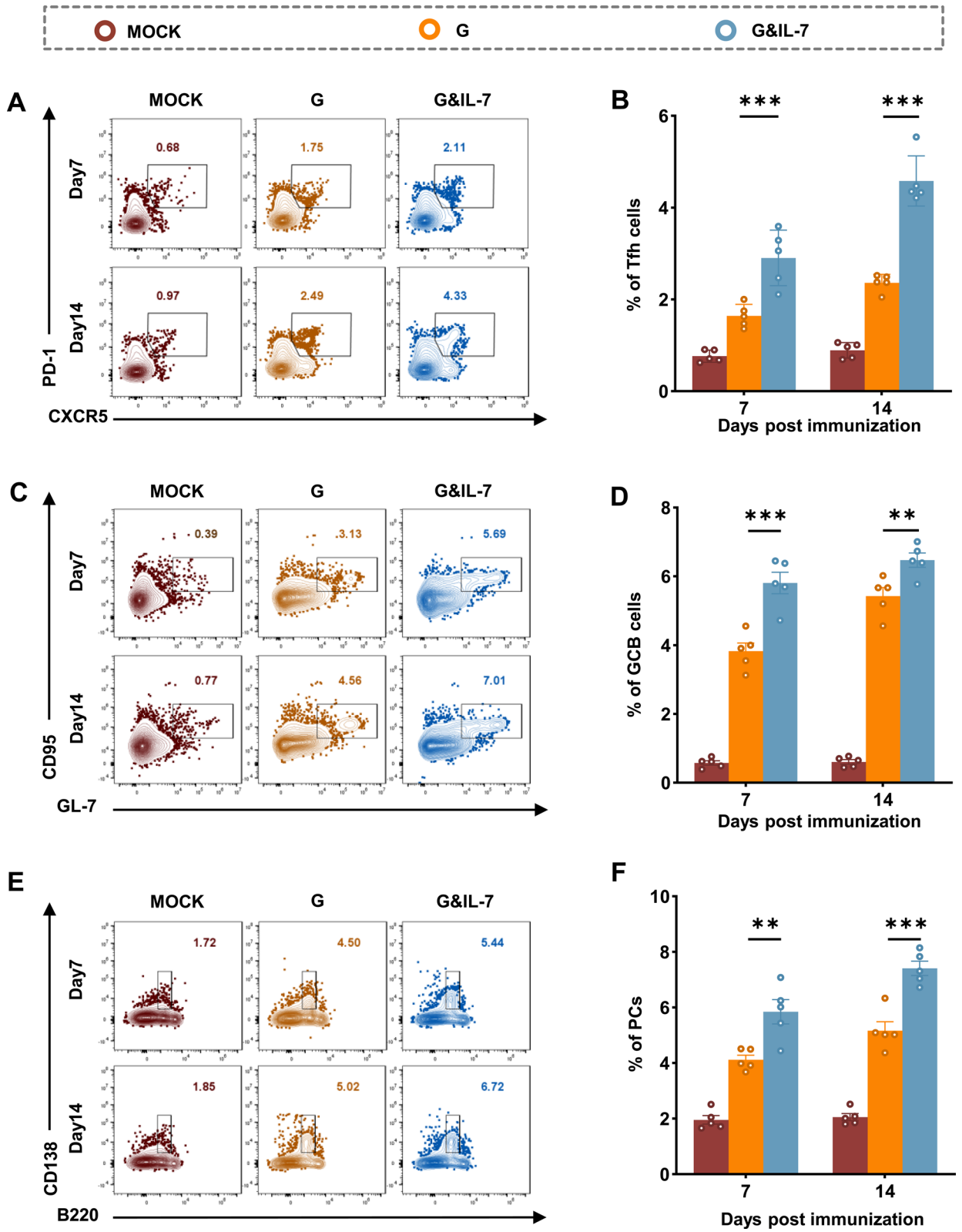

Fig. 4 (See legend on previous page.)

24 after inoculation, respectively, while the mice in the placebo group all died of RABV within 11 days (Fig. 6F). In both vaccinated groups, there was a gradual increase in body weight after a temporary decline, whereas the negative control group showed a sustained decrease in body weight (Fig. 6B, E). These results demonstrate that G&IL-7 mRNA provides long-term prophylactic efficacy against lethal RABV challenge.

An acute toxicity assay was performed to preliminarily assess the safety profile of G&IL-7 mRNA vaccine. Serum samples collected 24 h after vaccine administration were used to assess the levels of several key cytokines and biochemical indicators. The results indicated that the levels of IL-1β, TNF-α, and IFN-γ remained unchanged, while IL-6, a cytokine crucial for early Tfh cell differentiation in mice [39], showed a modest increase in the groups vaccinated with G&IL-7 mRNA or G mRNA (Fig. S6A). Blood biochemical parameters, including ALT, AST, CREA, and TP, remained within normal physiological ranges (Fig. S6B). Furthermore, hematoxylin and eosin (H&E) staining of major organ sections revealed no significant pathological damage (Fig. S6C). These data provide preliminary evidence regarding the safety profile of the G&IL-7 mRNA vaccine.

A SARS-CoV-2 mRNA vaccine incorporated with IL-7 elicits potent immune responses

SARS-CoV-2 infection poses a substantial global health threat, emphasizing the critical importance of vaccines targeting this virus [40, 41]. To demonstrate the potential of the IL-7 mRNA in enhancing immunogenicity across diverse antigens, we developed an mRNA vaccine encoding the spike (S) protein of SARS-CoV-2 (Fig. 7A). After transfecting HEK-293T cells with LNP-encapsulated S mRNA, IL-7 mRNA or S&IL-7 mRNA, the expression of S and IL-7 was confirmed (Fig. 7B). Following this, IL-7 mRNA was incorporated as an adjuvant in S mRNA to assess its adjuvant effect in murine models. To select the optimal IL-7 mRNA dose, we conducted experiments with different dose gradients and ultimately chose 10 μg as the study dose (Fig. S7). Mice were divided into 2 groups, after immunizing with S mRNA and S&IL-7 mRNA for 4 weeks, respectively, a booster immunization was administered with the same dosage, serum samples were collected for detection of antibodies against SARS-CoV-2 (Fig. 7C). We utilized ELISA to detect S-specific IgG, and the results revealed that the IgG levels in the S&IL-7 mRNA group were higher than those in the S mRNA group during the week 4 of primary immunization and the week 2 and week 4 of booster immunization (Fig. 7D–G). Additionally, to further assess the quality of antibodies, IgG2a and IgG1 were measured using ELISA. The findings demonstrated that S&IL-7 mRNA induced elevated IgG2a (Fig. 7H) and IgG1 (Fig. 7I) levels at week 4 post booster immunization. Subsequently, a pseudovirus neutralization assay was employed to evaluate the anti-SARS-CoV-2 neutralizing antibodies (nAbs) in the serum of vaccinated mice. The results indicate that, from weeks 2 to 5 post-booster immunization, S&IL-7 mRNA induced higher $pVNT_{50}$ (pseudovirus 50% neutralization titers) compared to S mRNA alone (Fig. 7J). Moreover, at week 3 post-booster immunization, the $pVNT_{50}$ of S&IL-7 mRNA reached 2.8 times that of S mRNA. Overall, upon comparing the levels of IgG, IgG1 and IgG2a levels as well as $pVNT_{50}$, S&IL-7 mRNA induced a more robust immune response than S mRNA.

Discussion

With advancements in delivery systems represented by LNP, the application of mRNA vaccines is becoming increasingly widespread. Compared to traditional vaccines, mRNA vaccines have several advantages, including ease of manufacturing, rapid production, and favorable safety profiles. However, a challenge faced by mRNA vaccines is that the immune response induced by individual mRNA vaccines may be insufficient [42]. Previously, it has been observed that patients who received Pfizer's and Moderna's SARS-CoV-2 vaccines based on LNP technology experienced a gradual decline in immunity after vaccination, highlighting the need for further improvement of mRNA vaccines to achieve sustained immunity [43–45]. From the perspective of

(See figure on next page.)

Fig. 5 IL-7 facilitates the secondary antibody responses in mice. **A** Representative flow cytometric plots of MBCs in spleen cells. At 6 weeks post primary-immunization, spleens cells were stained with markers specific to MBCs ($B220^+IgD^-CD273^+CD38^+$). **B** Statistical analyses were conducted on $B220^+IgD^-CD273^+CD38^+$ MBCs plots (n = 5). **C** Experimental design schematic depicting the immunization protocol. C57BL/6 mice were immunized with G mRNA, G&IL-7 mRNA, or PBS. After 24 weeks, all groups received a booster dose of the same vaccine formulation. **D** Representative flow cytometric plots of PCs in BM cells. At 2 weeks after booster-immunization, BM cells were stained with markers specific to PCs ($B220^{low}CD138^+$). **E** Statistical analyses were conducted on $B220^{low}CD138^+$ PCs plots (n = 5). **F** Representative images from ELISpot assays were obtained. LNs cells were prepared at 2 weeks after booster-immunization, and the RABV-specific ASCs were quantified using the ELISpot assay. **G** Statistical analysis was conducted on the quantity of RABV-specific ASCs (n = 4). **H** The RABV IgG antibody was detected using ELISA before and after the booster dose (14 dpi) (n = 10). **I** VNA titers were assessed using fluorescent antibody virus neutralization assays before and after the booster dose (14 dpi)

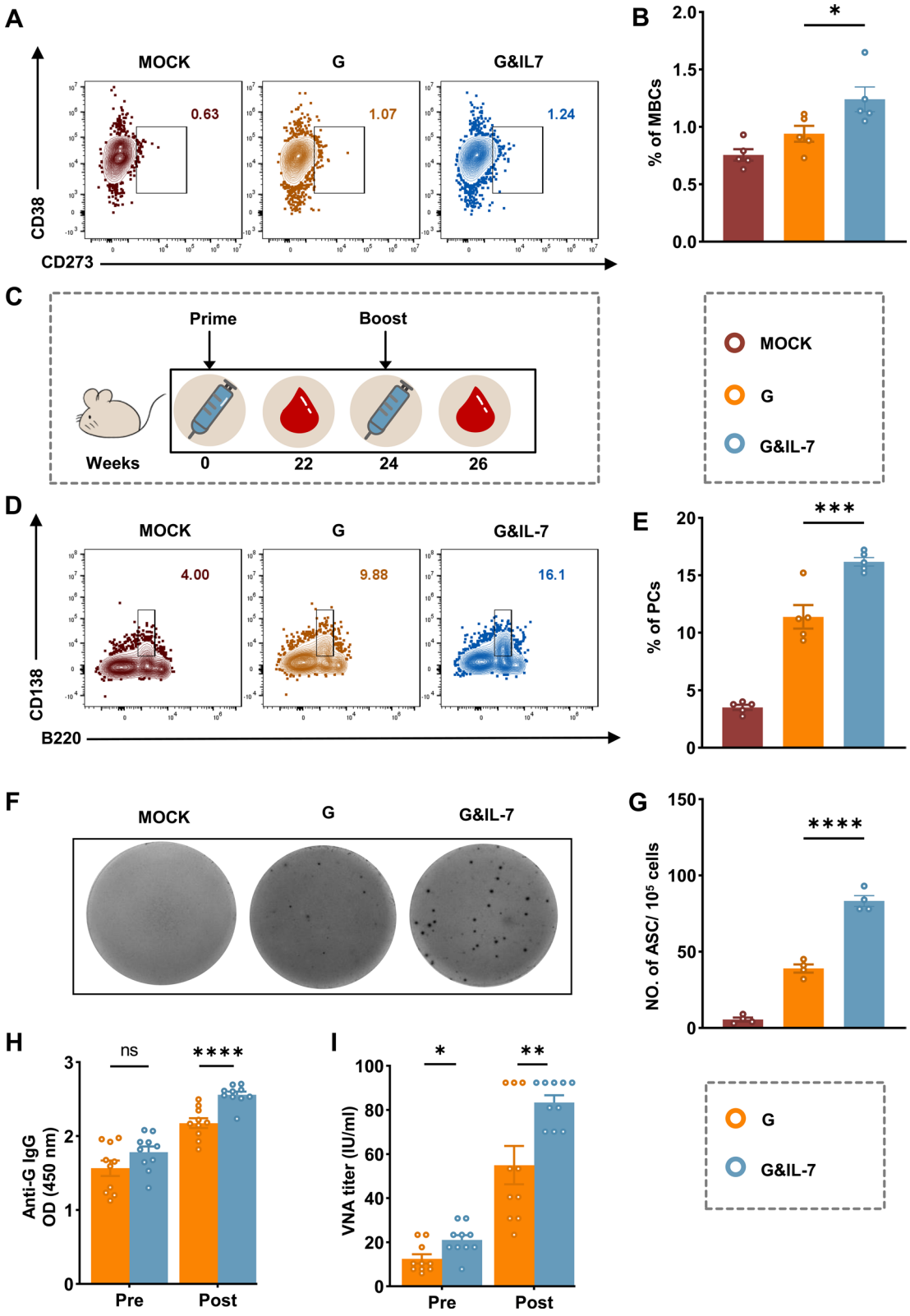

Fig. 5 (See legend on previous page.)

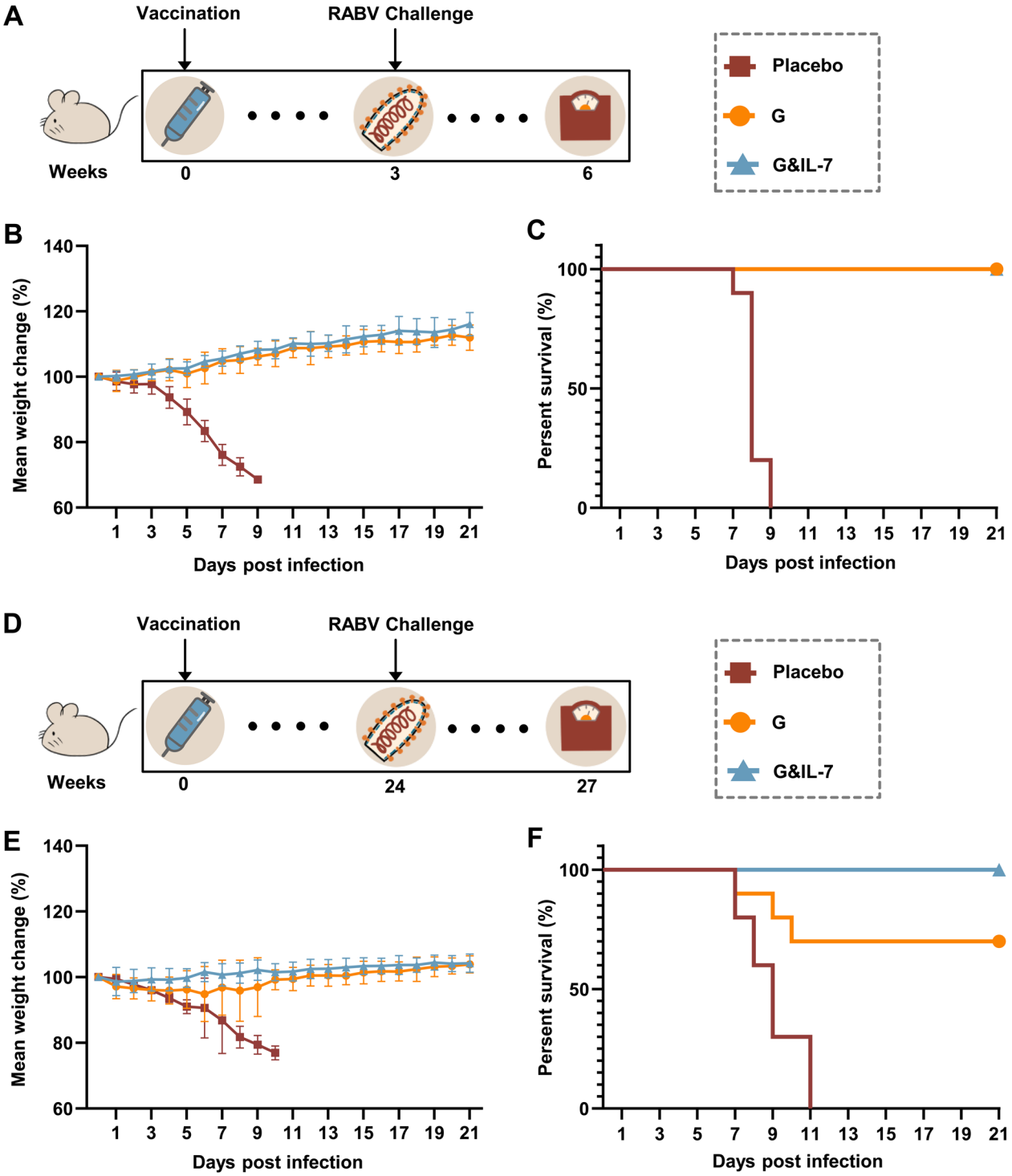

Fig. 6 A RABV mRNA vaccine expressing IL-7 induces durable antibody production and provides long-term protection. **A**, **D** Experimental design. 3 weeks (**A**) or 24 weeks (**D**) after immunization of mice with G mRNA, G&IL-7 mRNA, or PBS, an intracerebral injection of 50 LD_{50} of the virulent RABV strain CVS-24 was administered. **B**, **E** Changes in body weight are presented with error bars indicating the means ± standard deviation (SD). **C**, **F** Survival rates. Intergroup differences in survival rates were assessed using a log-rank test

reducing side effects and costs, this requires increasing the immunogenicity of mRNA vaccines without increasing or decreasing the vaccine dose. To elicit the optimal immune response, mRNA vaccines need to utilize appropriate adjuvants [42]. Here, we report an adjuvant strategy demonstrating that IL-7 mRNA can serve as an adjuvant for mRNA vaccines. By co-encapsulating with antigen mRNA in LNPs, it synergistically enhances the strength and durability of the immune response induced by mRNA vaccines.

Loading both antigen and adjuvant into a single vaccine formulation shows promise for enhancing vaccination outcomes [19, 46]. When applying this strategy to mRNA vaccines, adjuvant mRNA and antigen mRNA can be co-encapsulated into the delivery vehicle through simple mixing. Our previous research demonstrated that incorporating IL-7 into the recombinant RABV genome significantly enhances vaccine immunogenicity and induces durable humoral responses [47]. Additionally, IL-7 overexpression was found to boost the immune response in recombinant canine distemper virus vaccines [48]. Similarly, other studies have shown that co-delivery of mouse Fc-fused IL-7 with inactivated influenza vaccines enhances antibody responses [21, 49]. Moreover, strategies such as cloning IL-7 into DNA vaccines, co-delivering IL-7 DNA with DNA vaccines, or fusing IL-7 with antigens have been found to enhance immune responses across various vaccine platform [21, 50–53]. These findings demonstrate the application of IL-7 as an adjuvant in vaccines. While IL-7 has shown promise as an adjuvant in protein and DNA vaccines, its application in mRNA vaccines has not been shown to date. Using RABV G and SARS-CoV-2 S proteins as model antigens, we demonstrated that the co-immunization of G mRNA + IL-7 mRNA or S mRNA + IL-7 mRNA can induce potent antibody responses compared to mRNA encoding only G or S proteins. Consistent with previous reports, co-delivery of IL-7 mRNA significantly enhances the expansion of Tfh cells and GC B cells, as well as promotes the generation of plasma cells. Transcriptomic analysis of mouse inguinal lymph nodes post-vaccination also revealed significant enrichment of pathways associated with cell proliferation. Our study further expands the application potential of IL-7 as an adjuvant for mRNA vaccines.

IL-7 primarily influences the development of B cells, T cells, and dendritic cells by activating the JAK-STAT and PI3K-Akt signaling pathways [27, 28]. Previous studies have shown that IL-7 enhances STAT5 transcriptional activity, promoting Glut1 translocation and glucose uptake, which helps prevent T cell apoptosis and sustain T cell homeostasis [54]. Additionally, IL-7-mediated STAT5 activation plays a critical role in the survival of naïve CD4 T cells, further highlighting the importance of IL-7 in maintaining immune balance [55]. Therefore, we focused on the JAK-STAT pathway and investigated the expression of key genes and proteins associated with this signaling pathway. The upregulation of key genes and verification of protein phosphorylation indicate the role of IL-7 in mediating JAK-STAT signaling, consistent with previous studies [31, 32, 54–56]. However, the lymph node microenvironment is highly complicated, encompassing a diverse array of cell types, not all of which may respond to IL-7 signaling [57, 58]. Consequently, elucidating the mechanisms by which IL-7 extends humoral immune responses necessitates the use of more advanced technologies, such as single-cell techniques, for further investigation into its role in immune modulation.

The decline in vaccine-induced antibody titers increases the risk of breakthrough infections [11, 18, 59, 60]. To enhance the durability of immune responses, various strategies have been adopted, one of which is the use of multi-dose vaccinations. Currently licensed inactivated rabies vaccines have demonstrated acceptable efficacy and tolerability [61]. However, they are one of the most expensive vaccines on the market, requiring two to five doses depending on the regimen followed and whether the vaccine is administered before or after exposure [5, 14, 62]. In our previous work, effective protection with a single-dose RABV mRNA vaccine was achieved by increasing the translation level of the mRNA vaccine antigen, resulting in significantly enhanced immunogenicity [11]. Additionally, while the clinical trials of SARS-CoV-2 mRNA candidate vaccines have adopted a two-dose regimen, single-dose nucleoside-modified

(See figure on next page.)

Fig. 7 A SARS-CoV-2 mRNA vaccine incorporated with IL-7 elicits potent immune responses. **A** Schematic diagram of nucleoside-modified mRNA, encoding the full-length S protein. *S* spike protein of SARS-CoV-2, *SP* signal peptide. **B** HEK-293T cells were transfected with LNP-encapsulated S mRNA (2 μg), IL-7 mRNA (1 μg) or S&IL-7 mRNA (2 μg S mRNA + 1 μg IL-7 mRNA). After 24 h, Western blotting was performed to measure the expression levels of S and IL-7 in the cell lysates (n = 3). **C** Experimental design. Mice were vaccinated with 20 μg of S mRNA encapsulated in LNP or 10 μg of IL-7 mRNA co-encapsulated with 20 μg of S mRNA in LNP. After 4 weeks of primary immunization, a booster immunization was administered using the same dose as the primary immunization, and serum samples were collected. **D**–**G** SARS-CoV-2 S protein-binding IgG titers were detected using ELISA (n = 8). **H**, **I** SARS-CoV-2 S protein-binding IgG2a (**H**) and IgG1 (**I**) titers in mice following booster immunization (n = 8). **J** SARS-CoV-2 neutralizing antibodies against the original Wuhan strain in mice following booster immunization were detected using pseudovirus neutralization assay (n = 8)

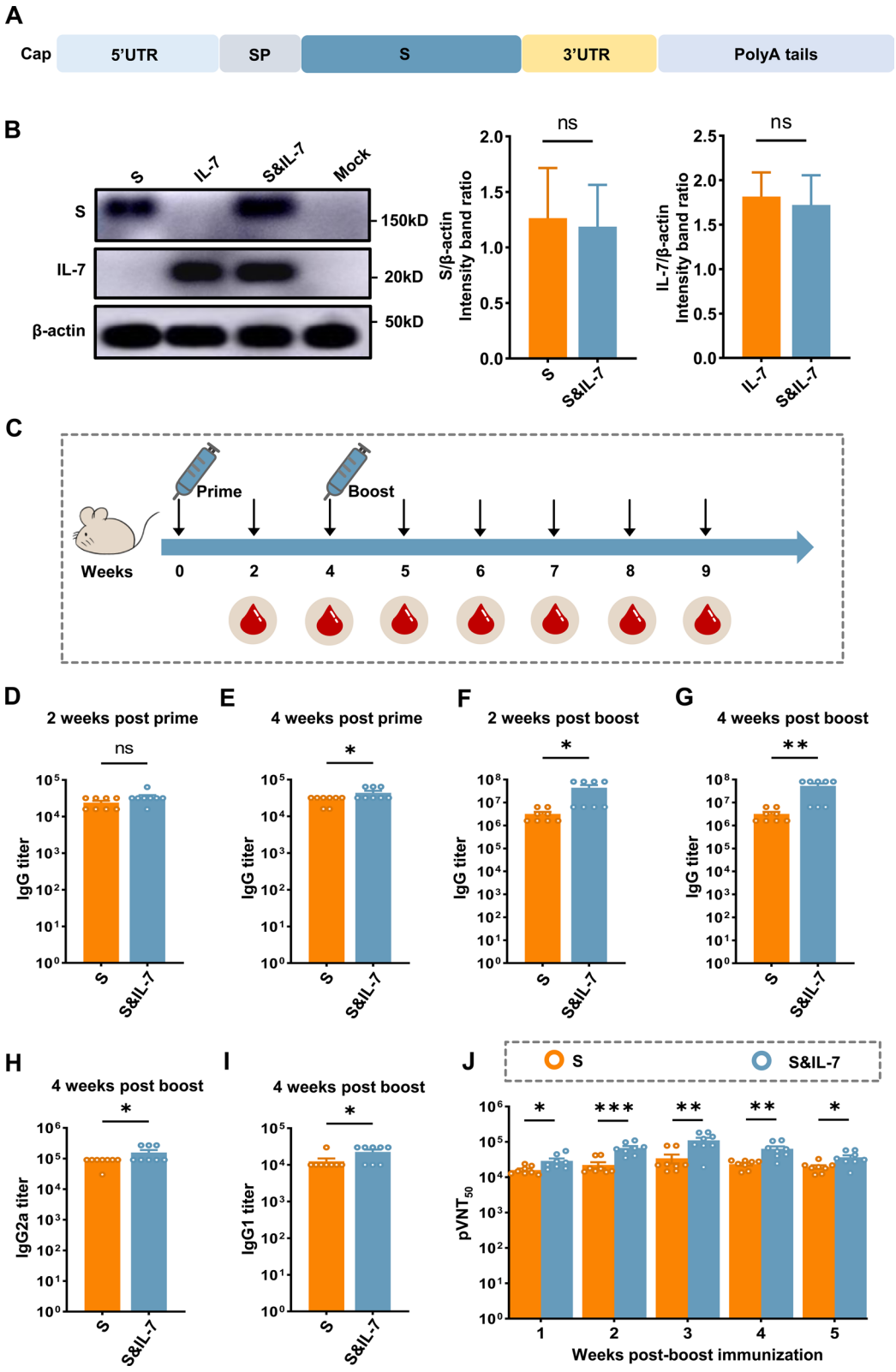

Fig. 7 (See legend on previous page.)

mRNA vaccine administration has been demonstrated to provide sufficient protection against Zika virus challenge in non-human primates [24]. Increasing the dose not only leads to increased costs but also complicates the vaccination process, making it difficult for underserved areas to fully comply with the complete vaccination schedule and increasing patient discomfort [5, 6].

IL-7 mRNA, through the synergistic immunogenicity induced with antigen mRNA, allows us to adopt a single-dose vaccination approach in our regimen. Surprisingly, the single-dose G mRNA + IL-7 mRNA vaccine not only significantly increases antibody levels but also effectively enhances the durability of the antibody response. Previous studies have found that long-term protection against lethal influenza virus infection can be achieved by intranasal introduction of fusion IL-7 [49]. Our research indicates that the high levels of RABV virus-neutralizing antibody induced by the G mRNA + IL-7 mRNA vaccine are maintained for at least 6 months, potentially longer, as RABV virus-neutralizing antibody titers remain stable, thus providing significant long-term protection against RABV infection. A RABV challenge trial conducted 6 months after vaccination confirmed this, demonstrating that the single-dose G mRNA + IL-7 mRNA vaccine can protect mice from lethal RABV challenge, consistent with high antibody levels. Additionally, we observed that IL-7 induces stronger immune memory, as levels of memory B cells remained higher 6 weeks after vaccination. Sequencing results also showed a significant upregulation of the cell anti-apoptosis pathway after IL-7 mRNA vaccination. Following immune enhancement, IL-7 induced more plasma cells and antibody-secreting cells production, ensuring rapid initiation of the immune response in mice, consistent with the antibody levels generated by the G mRNA + IL-7 mRNA vaccine. These results demonstrate the role of IL-7 as an mRNA vaccine adjuvant in reducing vaccination doses and prolonging the duration of immune responses.

Reducing vaccine dosage, minimizing the number of doses, and improving vaccination routes are the key concerns in vaccine development. The success of mRNA vaccines has made it possible to address these issues, provided suitable adjuvants for mRNA vaccine are found. In this study, we reported an effective adjuvant strategy, demonstrating that IL-7 can significantly enhance the immune response induced by mRNA vaccines and prolong the duration of the immune response. However, the antibody detection period was confined to 6 months and IL-7 showed a stable antibody response during this period, additional research is required to determine if this response is maintainable for over a year or longer. While IL-7 can offer potential benefits as an adjuvant for mRNA vaccines, its safety issues may limit its broader application. Therefore, despite initial studies in mice not showing significant issues, further investigation is needed to comprehensively assess any potential risks. In conclusion, this study provides more options and possibilities for the development of more effective and durable mRNA vaccines.

Materials and methods

Animals and ethics statement

C57BL/6 and ICR female mice at the age of 6 to 8-week-old were purchased from the Centers for Disease Control of Hubei Province, China. All mice were bred and maintained within a controlled specific pathogen-free (SPF) facility at the Laboratory Animal Center of Huazhong Agricultural University. Mice demonstrating a reduction in their initial body weight of ≥ 25% were euthanized in accordance with humane protocols and recorded as deceased. The experimental protocol underwent review and received approval from the Scientific Ethics Committee of Huazhong Agricultural University, bearing the approval number HZAUMO-2023-0040.

Cells, viruses, and reagents

HEK-293T, BSR and BHK-ACE2 cell lines were cultured in Dulbecco's modified Eagle's medium (DMEM) (Merck, Cat. No# D5546) supplemented with 10% fetal bovine serum (FBS) (Gibco, Cat. No# 16000-044) and 1% penicillin–streptomycin (Gibco, Cat. No# 15140122), within a 5% CO_2 atmosphere at 37 °C in an incubator. The virulent strain CVS-24 of RABV was preserved in our laboratory as previously outlined [63]. The licensed commercial inactivated rabies vaccine purchased from Intervert International B.V. (Boxmeer, Netherlands) was used as a reference control. For simplicity, this vaccine is referred to as ITV in the paper. A 0.1 dose of the ITV vaccine was used in mice as a control, as previously described [18]. The procedures for preparing SARS-CoV-2 pseudovirus were executed in accordance with previously published methodologies [64]. Briefly, HEK-293T cells were transfected with a plasmid expressing the SARS-CoV-2 S protein and infected with G*ΔG-VSV pseudotyped virus. After infection, the uncoated ΔG-VSV genome expressed all enzymes and structural proteins from the VSV genome except the G protein, which was replaced by a luciferase (Luc) reporter gene. Cell supernatants were collected 24 h after infection and transfection, divided into aliquots, and cryopreserved at − 80 °C.

The antibodies labeled directly with fluorescein for flow cytometric analyses were purchased from BioLegend (CA, USA). FITC anti-mouse CD4 antibody (Cat. No. 100510), PE anti-mouse CD279 (PD1) antibody (Cat. No. 135206), and APC anti-mouse CD185 (CXCR5) antibody (Cat. No. 145506) were employed for the identification

of Tfh cells within the inguinal lymph nodes; FITC anti-mouse CD45R/B220 antibody (Cat. No.103206), 647 anti-mouse GL7 antibody (Cat. No. 144606), PE anti-mouse CD95 antibody (Cat. No. 152608) were employed for the identification of GC B cells within the inguinal lymph nodes; FITC anti-mouse CD45R/B220 antibody (Cat. No. 103206) and APC anti-mouse CD138 (Syndecan-1) antibody (Cat. No. 142506) were employed for the assessment of plasma cell numbers within the bone marrow (BMs); PE/Cy7 anti-mouse CD45R/B220 antibody (Cat. No. 103222), FITC anti-mouse IgD (Cat. No. 405703), PE anti-mouse CD273 (Cat. No. 107205) and APC anti-mouse CD38 antibody (Cat. No. 102712) were employed for the identification of memory B cells (MBCs) within the spleens. Anti-RABV G protein monoclonal antibody and RABV G protein was prepared following established protocols as previously outlined [61, 63]. The antibodies labeled with fluorescein isothiocyanate (FITC) targeting the RABV N protein were purchased from Fujirebio Diagnostics, Inc. (Malvern, PA). Anti-IL-7 antibody (Cat. No. ab84271) was purchased from Abcam (Cambridge, UK). Anti-JAK1 antibody (Cat. No. A18323), anti-STAT5 antibody (Cat. No. A5029) and anti-Phospho-STAT5 antibody (Cat. No. AP0887) were purchased from Abclonal (Wuhan, China). Anti-Phospho-Jak1 antibody (Cat. No. 3331) was purchased from Cell Signaling Technology (Danvers, MA, USA). The horseradish peroxidase (HRP)-conjugated goat anti-mouse IgG, IgG1, IgG2a, and IgG2b antibodies for enzyme-linked immunosorbent assay (ELISA) were procured from Boster (Wuhan, China). Ionizable cationic lipid (SM102) (Cat. No. 06040008800), PEG-lipid (Cat. No. 06020112402), cholesterol (Cat. No. 06040010300), and phosphatidylcholine (DSPC) (Cat. No. 06030001100) were purchased from SINOPEG Biotechnology Co., Ltd. (Xiamen, China).

mRNA synthesis

mRNA was synthesized in vitro using the T7 High Yield RNA Transcription Kit (Novoprotein, Cat. No# E137), incorporating N1-methylpseudouridine as a substitute for uridine. The linear DNA template serving as a substrate comprises both the 5′ and 3′ untranslated regions (UTRs). The Cap 1 Capping System (Novoprotein, Cat. No# M082) and Poly(A) Polymerase (Novoprotein, Cat. No# M012) were employed to add the Cap1 structure and a poly(A) tail, respectively, to the 5′ and 3′ ends of mRNA. The purification of mRNA products entails mixing with lithium chloride and incubating at − 20 °C for a minimum of 30 min. Subsequently, centrifugation at 10,000×*g* at 4 °C for 15 min is performed to collect the precipitate. The pellet is then washed three times with pre-chilled 70% ethanol and resuspended in RNase-free water. Following resuspension, the precipitate is stored at − 80 °C until further utilization.

LNP Formulation of the mRNA

The LNP-mRNA vaccine utilizes LNPs formulation to encapsulate the mRNA. The LNPs employed in this study were formulated by dissolving an ionizable cationic lipid, phosphatidylcholine, cholesterol, and DSPE-PEG2k at a ratio of 50:10:38.5:1.5 in anhydrous ethanol [65]. Meanwhile, mRNA was dissolved in a citrate buffer with a pH of 4 and a concentration of 50 mM. The LNP and mRNA were mixed at a volume ratio of 1:3 within a microfluidic device, followed by dilution of the LNP-mRNA formulations with a 35-fold volume of 1 × PBS buffer (pH 7.4) and subsequent concentration to an mRNA concentration of 0.1 mg/mL using 30 kD Amicon Ultra Centrifugal Filters (Millipore, Cat. No# UFC903096).

Nanoparticle characterization

Particle size (Dynamic Light Scattering, DLS) measurements were performed using a Zeta sizer Nano ZS instrument (Malvern Instrument Co., Ltd.). Nanoparticles were added to 1 cm test dishes at appropriate concentrations, followed by analysis using a dynamic light scattering instrument to ascertain particle size. Transmission electron microscopy (TEM) was conducted following the dilution of LNP-mRNA nanoparticle. Specifically, 10 μL aliquots were placed onto copper mesh and allowed to stand for 10 min. Following the removal of excess liquid using filter paper, the morphology of LNPs was inspected utilizing a transmission electron microscope (HITACHI) equipped with a field emission gun operating at 80 kV.

mRNA transfection in vitro

HEK-293T cells were seeded at a density of 4×10^5 cells per well in 24-well plates and incubated at 37 °C in 5% CO_2 atmosphere for 12 h. Subsequently, LNP-encapsulated mRNA was directly transfected into HEK-293T cells. At 24 h after transfection, cell lysates were collected using RIPA Lysis Buffer (Beyotime, Cat. No# P0013D), followed by a 30 min incubation on ice. After centrifugation at 10,000×*g*, the supernatant was combined with SDS-loading buffer.

Mouse vaccination and challenge

Mice aged 6–8 weeks were randomly allocated to specified groups. Mice were immunized via intramuscular (i.m.) injection with LNP-encapsulated G mRNA, G&IL-7 mRNA, S mRNA, S&IL-7 mRNA. The ITV vaccine and PBS were used as a control. A mouse challenge model using the virulent RABV strain CVS-24 has been previously described [61]. At either 3 weeks or 6 months post-immunization, mice were subjected to

an intracranial challenge with 30 μL of 50 LD_{50} (median lethal doses) of CVS-24. Subsequently, their body weights and mortality were monitored and recorded daily.

RABV virus-neutralizing antibody measurement

RABV virus-neutralizing antibody (VNA) titers were measured using the fluorescent-antibody virus neutralization (FAVN) assay, following previously described methods [66]. In brief, blood was collected from mice at specific time points, and the serum was subsequently separated and inactivated for 30 min at 56 °C. Test serum and standard serum were serially diluted in 96-well microplates. 100 μL of DMEM was dispensed into each well of a 96-well plate, followed by adding 50 μL of either test serum or standard serum to the first column, and then serial three-fold dilutions were performed. Each sample was added to four adjacent wells for analysis. A suspension of RABV (CVS-11) was added to each well, and the plates were then incubated at 37 °C for 1 h. Subsequently, 2×10^4 BSR cells were added to each well, followed by further incubation at 37 °C for 72 h. Samples were then fixed with 80% ice-cold acetone for 30 min and stained with FITC-conjugated antibodies targeting the RABV N protein. Fluorescence was observed utilizing an Olympus IX51 fluorescence microscope (Olympus, Tokyo, Japan). Fluorescence values were compared with reference serum values acquired from the National Institute for Biological Standards and Control in Hertfordshire, UK. Following this, the results were standardized and quantified as international units per milliliter (IU/mL).

ELISA analysis of antibody titers

ELISAs were performed to determine antibody, following established protocols [67]. In brief, serum samples were collected and subsequently inactivated at 56 °C for 30 min. ELISA plates were incubated overnight at 4 °C with purified RABV virion, which were diluted to a concentration of 500 ng per well in a protein coating buffer (5 mM Na_2CO_3, pH 9.6). After incubating overnight at 4 °C, the plates were washed three times and then blocked for 1 h at 37 °C. The serum was subsequently diluted in PBST containing 5% (wt/vol) skim milk at dilutions of 1:2,000 for IgG, 1:100 for IgG1, and 1:200 for IgG2a and IgG2b. Subsequently, 100 μL of the diluted serum was dispensed into the plates and incubated at 37 °C for 1 h. After washing the plates three times with PBST, 100 μL of horseradish peroxidase (HRP)-conjugated goat anti-mouse IgG, IgG1, IgG2a, or IgG2b was added to each well and incubated for 45 min at 37 °C. After the incubation, the plates were washed three times. Subsequently, 100 μL of tetramethylbenzidine (TMB) substrate (Biotime Biotechnology, Shanghai, China) was added to each well to initiate a chromogenic reaction, and the plates were allowed to incubated at 37 °C for 5 min before the addition of 50 μL of 2 M H_2SO_4. Optical densities were measured at 450 nm using a SpectraMax 190 spectrophotometer (Molecular Devices, CA, USA).

The SARS-CoV-2 S-specific IgG, IgG1, and IgG2a antibody were measured by ELISA. ELISA plates were coated overnight at 4 °C with 100 μL of a solution containing 2 ng/μL of SARS-CoV-2 S protein (Vazyme, Cat. No# CG202-01) diluted in coating buffer. After blocking the plates for 1 h, the diluted serum was added and incubated for 1 h, followed by 3 washes with PBST. Subsequently, plates were treated with horseradish peroxidase (HRP)-conjugated rabbit anti-mouse IgG, IgG1, or IgG2a, and incubated at 37 °C for 60 min. The subsequent chromogenic steps followed the previously described protocol. The endpoint titers were defined as the highest reciprocal dilution of serum to yield an absorbance greater than 2.1-fold of the background values.

Pseudovirus neutralization assay

SARS-CoV-2 neutralizing antibody titers were assessed following established protocols [64]. In brief, the mouse serum was serially diluted and then mixed with a specific quantity (ranging from 325 to 1300 $TCID_{50}$/mL) of pseudotyped virus for 1 h at 37 °C. After that, BHK-ACE2 cells were added to each well, followed by further incubation at 37 °C for 24 h. A negative control using DMEM was incorporated for comparative analysis. Subsequently, the supernatant was removed, and a luciferase substrate as dispensed into each well. The mixture was then left to incubate in the dark at room temperature for 2 min. Luciferase activity was quantified using a Spark® Multimode microplate reader (TECAN, Swiss). The $pVNT_{50}$ was characterized as the dilution fold achieving over 50% inhibition of pseudotyped virus infection relative to the control group.

Flow cytometry (FCM) and ELISpot assay

T follicular helper (Tfh) cells, Germinal Center B (GC B) cells, memory B cells (MBCs), and plasma cells (PCs) obtained from inguinal lymph nodes (LNs), spleens or bone marrows (BMs) were examined using flow cytometry, following established procedures [61]. In brief, LNs, spleens and BMs from mice were harvested, and solid tissues were gently homogenized in pre-cooled PBS (pH 7.4). The cells were suspended in PBS containing 0.2% BSA (w/v), filtered through a 40-mm nylon filter into a tube, centrifuged, and then washed with PBS containing 0.2% BSA. After removing red blood cells using lysis buffer (catalog number 555899, BD Biosciences Inc., Franklin Lakes, NJ, USA), the cells were washed twice with PBS containing 0.2% BSA and then resuspended.

Subsequently, the resuspended cells were counted, and 1×10^6 cells were stained with fluorescence-labeled antibodies. After incubation at 4 °C for 30 min, the cells were washed twice with PBS containing 0.2% BSA. Finally, data acquisition and analysis were conducted utilizing a BD FACSVerse flow cytometer (BD Biosciences, CA, USA) along with FlowJo software (TreeStar, CA, USA).

The ELISpot assay was conducted to evaluate the production of RABV-specific antibody-secreting cells in the inguinal lymph nodes [68]. Multiscreen HA ELISpot plates (Millipore, MA, USA) were coated with 500 ng of purified RABV virions per well and then incubated for 16 h at 4 °C. The coated plates were washed and subsequently blocked with RPMI 1640 supplemented with 10% FBS for 2 h at 37 °C. Cell suspensions from inguinal LNs were added to the blocked ELISpot plates and incubated at 37 °C for 24 h. Following this, the cells in the ELISpot plates underwent sequential incubation with biotin-conjugated mouse IgG antibody (Bethyl Laboratories, TX, USA) and streptavidin–alkaline phosphatase (Mabtech, Stockholm, Sweden), followed by color development using BCIP/NBT-plus (Mabtech, Stockholm, Sweden). The plates were scanned, and spots were quantified. Then, the plates underwent scanning and analysis using the Mabtech IRIS FluoroSpot/ELISpot reader, employing RAWspot technology for multiplexing at the single-cell level.

Statistical analyses

Statistical analyses were conducted using GraphPad Prism software version 9.0 (GraphPad Software, Inc., CA). For the survival rate assessments, survival curves were evaluated using the log-rank (Mantel-Cox) test. For other datasets, significant variances among groups were assessed using Student's *t*-test and one-way ANOVA followed by post-hoc tests. The notations used to denote significant distinctions between groups were as follows: $^{*}P<0.05$; $^{**}P<0.01$; $^{***}P<0.001$; $^{****}P<0.0001$; ns, no significant difference.

Supplementary Information

The online version contains supplementary material available at https://doi.org/10.1186/s12951-024-02993-5.

Supplementary Material 1.

Acknowledgements
This study was partially supported by the National Key Research and Development Program of China (No. 2022YFD1800100) and the Fundamental Research Funds for the Central Universities (No. 2662023PY005). Sequencing service was provided by Bioyi Biotechnology Co., Ltd. Wuhan, China.

Author contributions
L.W and J.W planned and performed the experiments, analyzed the data, and wrote the manuscript; W.H, Z.W and Q.W performed the experiments; M.Z and Z.F planned the experiments, analyzed the data, and discussed the data; L.Z directed the study and wrote the manuscript. All authors reviewed the manuscript. Lead contact: Ling Zhao.

Availability of data and materials
No datasets were generated or analysed during the current study.

Declarations

Competing interests
The authors declare no competing interests.

Author details
[1]National Key Laboratory of Agricultural Microbiology, Huazhong Agricultural University, Wuhan 430070, China. [2]Hubei Hongshan Laboratory, Wuhan 430070, China. [3]Frontiers Science Center for Animal Breeding and Sustainable Production, Wuhan 430070, China. [4]Key Laboratory of Preventive Veterinary Medicine of Hubei Province, College of Veterinary Medicine, Huazhong Agricultural University, Wuhan 430070, China.

Received: 31 May 2024 Accepted: 5 November 2024
Published online: 16 November 2024

References

1. Li J, Liu Q, Liu J, Wu X, Lei Y, Li S, et al. An mRNA-based rabies vaccine induces strong protective immune responses in mice and dogs. Virol J. 2022;19(1):184. https://doi.org/10.1186/s12985-022-01919-7.
2. Rupprecht CE, Mshelbwala PP, Reeves RG, Kuzmin IV. Rabies in a postpandemic world: resilient reservoirs, redoubtable riposte, recurrent roadblocks, and resolute recidivism. Anim Dis. 2023;3(1):15. https://doi.org/10.1186/s44149-023-00078-8.
3. Fooks AR, Cliquet F, Finke S, Freuling C, Hemachudha T, Mani RS, et al. Rabies. Nat Rev Dis Prim. 2017;3:17091. https://doi.org/10.1038/nrdp.2017.91.
4. Hellgren F, Cagigi A, Arcoverde Cerveira R, Ols S, Kern T, Lin A, et al. Unmodified rabies mRNA vaccine elicits high cross-neutralizing antibody titers and diverse B cell memory responses. Nat Commun. 2023;14(1):3713. https://doi.org/10.1038/s41467-023-39421-5.
5. Warrell MJ. Current rabies vaccines and prophylaxis schedules: preventing rabies before and after exposure. Travel Med Infect Dis. 2012;10(1):1–15. https://doi.org/10.1016/j.tmaid.2011.12.005.
6. Tran CH, Kligerman M, Andrecy LL, Etheart MD, Adrien P, Blanton JD, et al. Rabies vaccine initiation and adherence among animal-bite patients in Haiti, 2015. PLoS Negl Trop Dis. 2018;12(11): e0006955. https://doi.org/10.1371/journal.pntd.0006955.
7. Ngugi JN, Maza AK, Omolo OJ, Obonyo M. Epidemiology and surveillance of human animal-bite injuries and rabies post-exposure prophylaxis, in selected counties in Kenya, 2011–2016. BMC Public Health. 2018;18(1):996. https://doi.org/10.1186/s12889-018-5888-5.
8. Cirelli KM, Crotty S. Germinal center enhancement by extended antigen availability. Curr Opin Immunol. 2017;47:64–9. https://doi.org/10.1016/j.coi.2017.06.008.
9. Miyauchi K, Adachi Y, Tonouchi K, Yajima T, Harada Y, Fukuyama H, et al. Influenza virus infection expands the breadth of antibody responses through IL-4 signalling in B cells. Nat Commun. 2021;12(1):3789. https://doi.org/10.1038/s41467-021-24090-z.
10. Alameh MG, Tombacz I, Bettini E, Lederer K, Sittplangkoon C, Wilmore JR, et al. Lipid nanoparticles enhance the efficacy of mRNA and protein subunit vaccines by inducing robust T follicular helper cell and humoral responses. Immunity. 2021;54(12):2877-2892.e7. https://doi.org/10.1016/j.immuni.2021.11.001.
11. Wan J, Wang Z, Wang L, Wu L, Zhang C, Zhou M, et al. Circular RNA vaccines with long-term lymph node-targeting delivery stability after lyophilization induce potent and persistent immune responses. MBio. 2024;15(1): e0177523. https://doi.org/10.1128/mbio.01775-23.

12. Amaya L, Grigoryan L, Li Z, Lee A, Wender PA, Pulendran B, et al. Circular RNA vaccine induces potent T cell responses. Proc Natl Acad Sci USA. 2023;120(20): e2302191120. https://doi.org/10.1073/pnas.2302191120.
13. Tai W, Yang K, Liu Y, Li R, Feng S, Chai B, et al. A lung-selective delivery of mRNA encoding broadly neutralizing antibody against SARS-CoV-2 infection. Nat Commun. 2023;14(1):8042. https://doi.org/10.1038/s41467-023-43798-8.
14. Lutz J, Lazzaro S, Habbeddine M, Schmidt KE, Baumhof P, Mui BL, et al. Unmodified mRNA in LNPs constitutes a competitive technology for prophylactic vaccines. NPJ Vaccines. 2017;2:29. https://doi.org/10.1038/s41541-017-0032-6.
15. Schnee M, Vogel AB, Voss D, Petsch B, Baumhof P, Kramps T, et al. An mRNA vaccine encoding rabies virus glycoprotein induces protection against lethal infection in mice and correlates of protection in adult and newborn pigs. PLoS Negl Trop Dis. 2016;10(6): e0004746. https://doi.org/10.1371/journal.pntd.0004746.
16. Alberer M, Gnad-Vogt U, Hong HS, Mehr KT, Backert L, Finak G, et al. Safety and immunogenicity of a mRNA rabies vaccine in healthy adults: an open-label, non-randomised, prospective, first-in-human phase 1 clinical trial. Lancet. 2017;390(10101):1511–20. https://doi.org/10.1016/S0140-6736(17)31665-3.
17. Aldrich C, Leroux-Roels I, Huang KB, Bica MA, Loeliger E, Schoenborn-Kellenberger O, et al. Proof-of-concept of a low-dose unmodified mRNA-based rabies vaccine formulated with lipid nanoparticles in human volunteers: a phase 1 trial. Vaccine. 2021;39(8):1310–8. https://doi.org/10.1016/j.vaccine.2020.12.070.
18. Wan J, Yang J, Wang Z, Shen R, Zhang C, Wu Y, et al. A single immunization with core-shell structured lipopolyplex mRNA vaccine against rabies induces potent humoral immunity in mice and dogs. Emerg Microbes Infect. 2023;12(2):2270081. https://doi.org/10.1080/22221751.2023.2270081.
19. Tockary TA, Abbasi S, Matsui-Masai M, Hayashi A, Yoshinaga N, Boonstra E, et al. Comb-structured mRNA vaccine tethered with short double-stranded RNA adjuvants maximizes cellular immunity for cancer treatment. Proc Natl Acad Sci USA. 2023;120(29): e2214320120. https://doi.org/10.1073/pnas.2214320120.
20. Fan N, Chen K, Zhu R, Zhang Z, Huang H, Qin S, et al. Manganese-coordinated mRNA vaccines with enhanced mRNA expression and immunogenicity induce robust immune responses against SARS-CoV-2 variants. Sci Adv. 2022;8(51): eabq3500. https://doi.org/10.1126/sciadv.abq3500.
21. Seo YB, Im SJ, Namkoong H, Kim SW, Choi YW, Kang MC, et al. Crucial roles of interleukin-7 in the development of T follicular helper cells and in the induction of humoral immunity. J Virol. 2014;88(16):8998–9009. https://doi.org/10.1128/JVI.00534-14.
22. Victora GD, Nussenzweig MC. Germinal centers. Annu Rev Immunol. 2022;40:413–42. https://doi.org/10.1146/annurev-immunol-120419-022408.
23. Tilsed CM, Sadiq BA, Papp TE, Areesawangkit P, Kimura K, Noguera-Ortega E, et al. IL7 increases targeted lipid nanoparticle-mediated mRNA expression in T cells in vitro and in vivo by enhancing T cell protein translation. Proc Natl Acad Sci USA. 2024;121(13): e2319856121. https://doi.org/10.1073/pnas.2319856121.
24. Pardi N, Hogan MJ, Pelc RS, Muramatsu H, Andersen H, DeMaso CR, et al. Zika virus protection by a single low-dose nucleoside-modified mRNA vaccination. Nature. 2017;543(7644):248–51. https://doi.org/10.1038/nature21428.
25. Li M, Fang E, Wang Y, Shi L, Li J, Peng Q, et al. An mRNA vaccine against rabies provides strong and durable protection in mice. Front Immunol. 2023;14:1288879. https://doi.org/10.3389/fimmu.2023.1288879.
26. Lian J, Ozga AJ, Sokol CL, Luster AD. Targeting lymph node niches enhances type 1 immune responses to immunization. Cell Rep. 2020;31(8): 107679. https://doi.org/10.1016/j.celrep.2020.107679.
27. McDonald PW, Read KA, Baker CE, Anderson AE, Powell MD, Ballesteros-Tato A, et al. IL-7 signalling represses Bcl-6 and the TFH gene program. Nat Commun. 2016;7:10285. https://doi.org/10.1038/ncomms10285.
28. Barata JT, Silva A, Brandao JG, Nadler LM, Cardoso AA, Boussiotis VA. Activation of PI3K is indispensable for interleukin 7-mediated viability, proliferation, glucose use, and growth of T cell acute lymphoblastic leukemia cells. J Exp Med. 2004;200(5):659–69. https://doi.org/10.1084/jem.20040789.
29. Corfe SA, Paige CJ. The many roles of IL-7 in B cell development; mediator of survival, proliferation and differentiation. Semin Immunol. 2012;24(3):198–208. https://doi.org/10.1016/j.smim.2012.02.001.
30. Hu Q, Bian Q, Rong D, Wang L, Song J, Huang HS, et al. JAK/STAT pathway: extracellular signals, diseases, immunity, and therapeutic regimens. Front Bioeng Biotechnol. 2023;11:1110765. https://doi.org/10.3389/fbioe.2023.1110765.
31. Shi L, Xu Z, Yang Q, Huang Y, Gong Y, Wang F, et al. IL-7-mediated IL-7R-JAK3/STAT5 signalling pathway contributes to chemotherapeutic sensitivity in non-small-cell lung cancer. Cell Prolif. 2019;52(6): e12699. https://doi.org/10.1111/cpr.12699.
32. Rochman Y, Kashyap M, Robinson GW, Sakamoto K, Gomez-Rodriguez J, Wagner KU, et al. Thymic stromal lymphopoietin-mediated STAT5 phosphorylation via kinases JAK1 and JAK2 reveals a key difference from IL-7-induced signaling. Proc Natl Acad Sci USA. 2010;107(45):19455–60. https://doi.org/10.1073/pnas.1008271107.
33. Allen CD, Okada T, Cyster JG. Germinal-center organization and cellular dynamics. Immunity. 2007;27(2):190–202. https://doi.org/10.1016/j.immuni.2007.07.009.
34. Victora GD, Nussenzweig MC. Germinal centers. Annu Rev Immunol. 2012;30:429–57. https://doi.org/10.1146/annurev-immunol-020711-075032.
35. Shlomchik MJ, Weisel F. Germinal center selection and the development of memory B and plasma cells. Immunol Rev. 2012;247(1):52–63. https://doi.org/10.1111/j.1600-065X.2012.01124.x.
36. Kroese FG, Wubbena AS, Seijen HG, Nieuwenhuis P. Germinal centers develop oligoclonally. Eur J Immunol. 1987;17(7):1069–72. https://doi.org/10.1002/eji.1830170726.
37. McHeyzer-Williams M, Okitsu S, Wang N, McHeyzer-Williams L. Molecular programming of B cell memory. Nat Rev Immunol. 2011;12(1):24–34. https://doi.org/10.1038/nri3128.
38. Laidlaw BJ, Cyster JG. Transcriptional regulation of memory B cell differentiation. Nat Rev Immunol. 2021;21(4):209–20. https://doi.org/10.1038/s41577-020-00446-2.
39. Crotty S. Follicular helper CD4 T cells (TFH). Annu Rev Immunol. 2011;29:621–63. https://doi.org/10.1146/annurev-immunol-031210-101400.
40. Zhang NN, Zhang RR, Zhang YF, Ji K, Xiong XC, Qin QS, et al. Rapid development of an updated mRNA vaccine against the SARS-CoV-2 Omicron variant. Cell Res. 2022;32(4):401–3. https://doi.org/10.1038/s41422-022-00626-w.
41. Fang E, Liu X, Li M, Zhang Z, Song L, Zhu B, et al. Advances in COVID-19 mRNA vaccine development. Signal Transduct Target Ther. 2022;7(1):94. https://doi.org/10.1038/s41392-022-00950-y.
42. Li B, Jiang AY, Raji I, Atyeo C, Raimondo TM, Gordon AGR, et al. Enhancing the immunogenicity of lipid-nanoparticle mRNA vaccines by adjuvanting the ionizable lipid and the mRNA. Nat Biomed Eng. 2023. https://doi.org/10.1038/s41551-023-01082-6.
43. Polack FP, Thomas SJ, Kitchin N, Absalon J, Gurtman A, Lockhart S, et al. Safety and efficacy of the BNT162b2 mRNA Covid-19 vaccine. N Engl J Med. 2020;383(27):2603–15. https://doi.org/10.1056/NEJMoa2034577.
44. Baden LR, El Sahly HM, Essink B, Kotloff K, Frey S, Novak R, et al. Efficacy and safety of the mRNA-1273 SARS-CoV-2 vaccine. N Engl J Med. 2021;384(5):403–16. https://doi.org/10.1056/NEJMoa2035389.
45. Rosenblum HG, Gee J, Liu R, Marquez PL, Zhang B, Strid P, et al. Safety of mRNA vaccines administered during the initial 6 months of the US COVID-19 vaccination programme: an observational study of reports to the vaccine adverse event reporting system and v-safe. Lancet Infect Dis. 2022;22(6):802–12. https://doi.org/10.1016/S1473-3099(22)00054-8.
46. Fischer NO, Rasley A, Corzett M, Hwang MH, Hoeprich PD, Blanchette CD. Colocalized delivery of adjuvant and antigen using nanolipoprotein particles enhances the immune response to recombinant antigens. J Am Chem Soc. 2013;135(6):2044–7. https://doi.org/10.1021/ja3063293.
47. Li Y, Zhou M, Luo Z, Zhang Y, Cui M, Chen H, et al. Overexpression of interleukin-7 extends the humoral immune response induced by rabies vaccination. J Virol. 2017;91(7):10–128. https://doi.org/10.1128/JVI.02324-16.
48. Chen C, Zhou M, Yan XG, Chen YX, Cui M, Chen HC, et al. A recombinant canine distemper virus expressing interleukin-7 enhances humoral immunity. J Gen Virol. 2019;100(4):602–15. https://doi.org/10.1099/jgv.0.001247.

49. Kang MC, Choi DH, Choi YW, Park SJ, Namkoong H, Park KS, et al. Intranasal introduction of fc-fused interleukin-7 provides long-lasting prophylaxis against lethal influenza virus infection. J Virol. 2015;90(5):2273–84. https://doi.org/10.1128/JVI.02768-15.
50. Nanjappa SG, Walent JH, Morre M, Suresh M. Effects of IL-7 on memory CD8 T cell homeostasis are influenced by the timing of therapy in mice. J Clin Invest. 2008;118(3):1027–39. https://doi.org/10.1172/JCI32020.
51. Cui D, Zhang J, Zuo Y, Huo S, Zhang Y, Wang L, et al. Recombinant chicken interleukin-7 as a potent adjuvant increases the immunogenicity and protection of inactivated infectious bursal disease vaccine. Vet Res. 2018;49(1):10. https://doi.org/10.1186/s13567-017-0497-3.
52. Panebra A, Lillehoj HS. *Eimeria tenella* elongation factor-1alpha (EF-1alpha) coadministered with chicken IL-7 (chIL-7) DNA vaccine emulsified in montanide gel 01 adjuvant enhanced the immune response to *E. acervulina* infection in broiler chickens. Avian Dis. 2019;63(2):342–50. https://doi.org/10.1637/11976-092418-Reg.1.
53. Park SH, Song MY, Nam HJ, Im SJ, Sung YC. Codelivery of IL-7 augments multigenic HCV DNA vaccine-induced antibody as well as broad T cell responses in cynomolgus monkeys. Immune Netw. 2010;10(6):198–205. https://doi.org/10.4110/in.2010.10.6.198.
54. Wofford JA, Wieman HL, Jacobs SR, Zhao Y, Rathmell JC. IL-7 promotes Glut1 trafficking and glucose uptake via STAT5-mediated activation of Akt to support T-cell survival. Blood. 2008;111(4):2101–11. https://doi.org/10.1182/blood-2007-06-096297.
55. Seki Y, Yang J, Okamoto M, Tanaka S, Goitsuka R, Farrar MA, et al. IL-7/STAT5 cytokine signaling pathway is essential but insufficient for maintenance of naive CD4 T cell survival in peripheral lymphoid organs. J Immunol. 2007;178(1):262–70. https://doi.org/10.4049/jimmunol.178.1.262.
56. Palmer MJ, Mahajan VS, Trajman LC, Irvine DJ, Lauffenburger DA, Chen J. Interleukin-7 receptor signaling network: an integrated systems perspective. Cell Mol Immunol. 2008;5(2):79–89. https://doi.org/10.1038/cmi.2008.10.
57. Ozulumba T, Montalbine AN, Ortiz-Cardenas JE, Pompano RR. New tools for immunologists: models of lymph node function from cells to tissues. Front Immunol. 2023;14:1183286. https://doi.org/10.3389/fimmu.2023.1183286.
58. Fry TJ, Mackall CL. Interleukin-7: from bench to clinic. Blood. 2002;99(11):3892–904. https://doi.org/10.1182/blood.v99.11.3892.
59. Aldridge RW, Yavlinsky A, Nguyen V, Eyre MT, Shrotri M, Navaratnam AMD, et al. SARS-CoV-2 antibodies and breakthrough infections in the virus watch cohort. Nat Commun. 2022;13(1):4869. https://doi.org/10.1038/s41467-022-32265-5.
60. Gupta RK, Topol EJ. COVID-19 vaccine breakthrough infections. Science. 2021;374(6575):1561–2. https://doi.org/10.1126/science.abl8487.
61. Wang Z, Yuan Y, Chen C, Zhang C, Huang F, Zhou M, et al. Colloidal manganese salt improves the efficacy of rabies vaccines in mice, cats, and dogs. J Virol. 2021;95(23): e0141421. https://doi.org/10.1128/JVI.01414-21.
62. World Health O. WHO expert consultation on rabies. Second report. World Health Organ Tech Rep Ser. 2013;982:1–139, back cover.
63. Zhang C, Tian Y, Chen C, Wang Z, Pei J, Lin C, et al. Virus-like vesicles based on Semliki forest virus-containing rabies virus glycoprotein make a safe and efficacious rabies vaccine candidate in a mouse model. J Virol. 2021;95(20): e0079021. https://doi.org/10.1128/JVI.00790-21.
64. Nie J, Li Q, Wu J, Zhao C, Hao H, Liu H, et al. Quantification of SARS-CoV-2 neutralizing antibody by a pseudotyped virus-based assay. Nat Protoc. 2020;15(11):3699–715. https://doi.org/10.1038/s41596-020-0394-5.
65. Chen S, Tam YYC, Lin PJC, Sung MMH, Tam YK, Cullis PR. Influence of particle size on the in vivo potency of lipid nanoparticle formulations of siRNA. J Control Release. 2016;235:236–44. https://doi.org/10.1016/j.jconrel.2016.05.059.
66. Zhang Y, Wu Q, Zhou M, Luo Z, Lv L, Pei J, et al. Composition of the murine gut microbiome impacts humoral immunity induced by rabies vaccines. Clin Transl Med. 2020;10(4): e161. https://doi.org/10.1002/ctm2.161.
67. Rasalingam P, Rossiter JP, Mebatsion T, Jackson AC. Comparative pathogenesis of the SAD-L16 strain of rabies virus and a mutant modifying the dynein light chain binding site of the rabies virus phosphoprotein in young mice. Virus Res. 2005;111(1):55–60. https://doi.org/10.1016/j.virusres.2005.03.010.
68. Luo Z, Li Y, Zhou M, Lv L, Wu Q, Chen C, et al. Toll-like receptor 7 enhances rabies virus-induced humoral immunity by facilitating the formation of germinal centers. Front Immunol. 2019;10:429. https://doi.org/10.3389/fimmu.2019.00429.

Publisher's Note